Polystyrene-Based Single-Walled Carbon Nanotube Nanocomposite Thin Films: Dynamics of Structural Instabilities

Brian M. Besancon and Peter F. Green*

Department of Chemical Engineering and Texas Materials Institute, University of Texas at Austin, Austin, Texas 78712

Received May 19, 2004; Revised Manuscript Received September 7, 2004

ABSTRACT: Thin polystyrene (PS) liquid films supported by oxidized silicon (SiO_x/Si) substrates may be unstable or metastable, depending on the film thickness, h. In the metastable thickness regime, holes nucleate throughout the surface of the films and subsequently grow under the action of capillary forces. Recent studies show that the hole growth rate in thin PS films is suppressed with the addition of small concentrations of C_{60} fullerenes, due to pinning at the line of contact. We examined the hole growth dynamics in thin film polystyrenes with functionalized single-walled carbon nanotubes (PS-SWNT) supported by SiO_x/Si substrates. The hole growth velocities in PS films containing 0.75 wt % functionalized single-walled nanotubes, $V_{PS-SWNT}$, were appreciably slower than V_{PS}, the hole-growth velocities of holes in polystyrene films of the same thickness. Moreover, $V_{PS-SWNT}$ and V_{PS} decreased with decreasing film thickness, for $h < 50$ nm, with thickness dependencies which exceed theoretical predictions. In addition, $V_{PS}(h)/V_{PS-SWNT}(h)$ increased with decreasing h, for $h < 50$ nm, and approached a constant value for larger h. We show that the suppression of the hole-growth rates in the PS−SWNT films are associated with larger viscosities of the PS−SWNT films and that the film thickness-dependent velocities are associated with film thickness-dependent viscosities.

Introduction

Applications involving single-walled carbon nanotubes (SWNT's), which include sensors, catalytic films, and microelectronic devices, take advantage of the unique physical properties of these materials.[1−6] Polymers containing small weight fractions (∼1 wt %) of SWNT's have been shown to exhibit substantial improvements of their mechanical properties.[7−11] Uniform dispersion of the nanotubes is necessary to achieve significant property improvements. However, the dispersion cannot be achieved without chemical functionalization of the nanotubes, needed to increase their compatibility with the polymer host.[11−16] The nanotubes otherwise exhibit a propensity to aggregate and form ropes or bundles.[11,12]

Mitchell et al.[11] showed that ∼1 wt % functionalized SWNT's formed a percolated network throughout polystyrene (PS) hosts and that the viscoelastic response of this material, PS-SWNT, was fundamentally different from that of pure PS. Whereas the low-frequency elastic modulus, G', of the pure PS exhibited linear viscoelastic behavior (i.e., $G' \sim \omega^2$), the nanocomposite exhibited pseudo-solid-like behavior, $G' \sim \omega^0$. The viscosity of the new nanocomposite also increased appreciably. For example, the zero shear viscosity of PS nanocomposites containing 0.75 wt % functionalized SWNT was found to be approximately a factor of 3 larger than that of pure PS.[11]

Like bulk polymer-based nanocomposites, polymer thin film nanocomposites are of current scientific and technological interest. Film thickness-dependent phase transitions are exhibited by thin film polymer−polymer mixtures and by block copolymer films.[17−22] Changes of the glass transition temperatures[23−31] and viscosities[32,33] with decreasing film thickness also occur in thin polymer films. Interactions between the polymer segments and the external interfaces and entropic effects, associated with the packing of chains, are generally implicated for these thickness-dependent properties.

Apart from the finite size property-dependent effects manifested by polymer films, thin, supported, polymer films may be structurally destabilized due to long-range intermolecular interactions.[34−44] Stable, unstable, or metastable behavior is largely associated with the curvature of the free energy of interaction per unit area, $\partial^2\Phi/\partial h^2$, between the polymer/substrate and polymer/free surface interfaces, separated by a distance h. Φ is often referred to as an effective interface potential. Holes nucleate throughout the surface of films in the metastable thickness regime, and these holes grow under the influence of capillary forces. It has been shown that C_{60} fullerenes,[45] silica,[46] and carbon black[46] suppressed the hole growth velocity in polystyrene films supported by oxidized silicon wafers. The suppression is due to the segregation of these particles to the line of contact, resulting in pinning.[45,46] Cole et al.[47] showed that alkanethiol-coated spherical gold particles dispersed throughout poly(*tert*-butyl acrylate) films had the effect of reducing the hole growth velocities due largely to an increase of the viscosity of the films. The proposed mechanism for the increase of the viscosity is believed to be associated with the formation of gold−polymer aggregates, wherein the polymer chains create bridges between the gold particles.[47] Computer simulations of polymer−filler systems indicate that dewetting rates should be affected by the mobility of the filler particles, by the interactions between the filler particles and the polymer, and by the size of the filler particles.[48]

In this paper we examine the effect of functionalized single-walled carbon nanotubes on the hole growth velocities in thin polystyrene (PS) films in the thickness range 25 nm $< h <$ 60 nm, supported by oxidized silicon wafers. The hole growth velocities, $V_{PS-SWNT}$, in the PS−SWNT nanocomposite films containing 0.75 wt % SWNTs were reduced by a factor of 5 compared to V_{PS}, the growth velocities in pure PS films. We show that this reduction is associated with the larger viscosities of the

10.1021/ma049008+ CCC: $30.25
Published on Web 12/14/2004

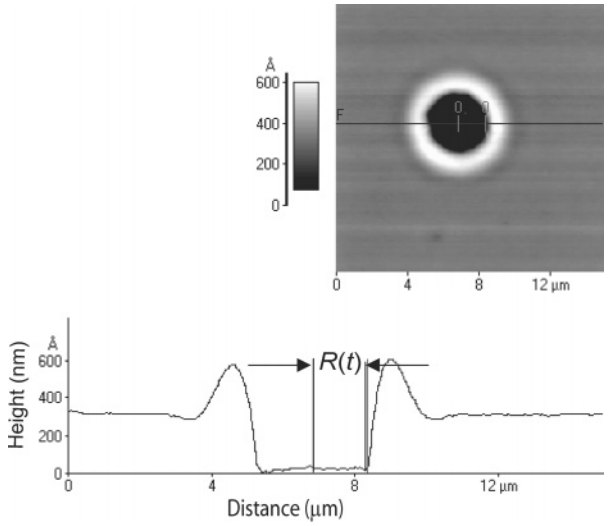

Figure 1. A typical AFM image of a hole is shown, accompanied by a line scan of the rim profile in which the radius of the hole is identified.

PS−SWNT films. Second, both $V_{PS-SWNT}$ and V_{PS} increased with decreasing h for $h < 50$ nm, at a rate far in excess of predictions based on theory; the velocities became independent of h for larger values of h. The film thickness dependence of the growth velocities is associated with film thickness-dependent viscosities. Finally, $V_{PS}/V_{PS-SWNT}$ increased with decreasing h for $h < 50$ nm.

Experimental Section

Nanocomposite materials of polystyrene (PS) of molecular weight 152 kg/mol functionally attached to 4-(10-hydroxydecyl)benzoate modified single-walled carbon nanotubes (SWNT) were used in this study. There is one functional group per every 66 carbon units. Details of the SWNT functionalization procedures as well as further information regarding the characterization of the nanocomposites may be found in refs 11−15. The diameter of the SWNT's was roughly 0.7 nm with an average tube length of ~1 μm.[16] Three series of samples were prepared. Films of PS containing 0.75 wt % functionalized SWNT (PS-SWNT) in the thickness range 25−65 nm were prepared by spin-coating solutions of PS-SWNT in toluene onto silicon wafers. The wafers were purchased from Wafer World, Inc. The wafers had a native oxide layer thickness of 1.5 nm, as measured by ellipsometry. A second series of nanocomposite thin films containing 3 wt % unfunctionalized SWNT's mixed with PS of the same molecular weight were also prepared. The third series of films consisting of pure PS of the same molecular weight used for to make the nanocomposites were prepared. The polystyrenes were purchased from Polymer Source.

After spin-casting, the average film thicknesses were measured using ellipsometry. Analyses of the topographies of the films were performed using scanning force microscopy (Autoprobe CP atomic force microscope from TM Microscopes). Ex-situ SFM scans were made employing the contact mode. Each film was scored after deposition to expose the underlying substrate so that the local film thickness could be determined from the SFM scans of the edges. The films were subsequently annealed at 170 °C under vacuum and periodically quenched and analyzed using SFM.

Figure 1 shows the morphology of a typical hole that develops in films in this thickness range; each hole is surrounded by a circular, stable, outer rim which increases in size as the hole grows. As discussed in an earlier publication, the rims surrounding holes in thinner PS films ($h < 24$ nm) of this molecular weight are unstable and form fingers.[49,50] The holes in these films increase in size and eventually impinge and subsequently approach a final stage characterized by large macroscopic droplets and small regions of tiny nanoscale droplets ~1 nm in height. The contact angles of the macroscopic droplets were $\theta_{PS-SWNT} = 32 \pm 2°$ in all samples examined. The time dependencies of the hole radii in different films are shown in Figure 2.

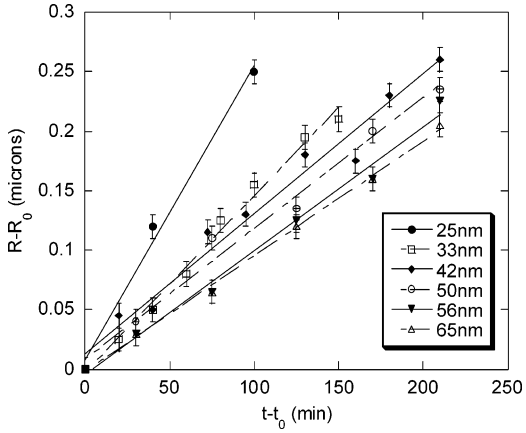

Figure 2. Hole radius as a function of time is shown for different film thicknesses of 0.75 wt % functionalized SWNT composites.

Results and Discussion

The structural destabilization of thin films is reasonably well understood. The free energy of interaction per unit area between the liquid/substrate and liquid/free surface interfaces separated by a distance h is determined by a combination of short and long-ranged intermolecular interactions. These are often represented by an effective interface potential, which has two contributions $\Phi = -A_{svl}/12\pi h^2 + \delta(h)$, where the first term describes the long-range contribution to the interaction; A_{svl} is the Hamaker constant.[34] The second term, $\delta(h)$, describes the short-range interactions.[34−38] A net attraction exists between the solid−liquid and liquid−vacuum interfaces when the Hamaker constant is positive. For the Si/SiO_x/PS/vacuum system, the effective Hamaker constant is positive, and thin PS liquid films are typically unstable or metastable, depending on the value of h.[32,33,36,37,39,40−43,50]

The nucleation of holes in the substrate occurs with the formation of a local depression in the film. This local depression penetrates into the film and impinges the substrate.[42] When a hole forms on the substrate, capillary forces are responsible for growth (negative spreading coefficient, S).[44,51] As a hole grows, a rim develops at the perimeter due to the accumulation of chains.[33,44] The driving force for hole growth is opposed by two processes: the dissipation of energy within the film due to viscous resistance and by the frictional resistance at the substrate/liquid interface. If friction at the substrate/liquid interface is the dominant mode of dissipation, then for small rim widths the velocity of growth is given by[43,44]

$$V \approx \frac{|S|}{\eta}\left(\frac{b}{h_0}\right)^{1/2} \quad (1)$$

In eq 1, η is the viscosity and b is the extrapolation length; b is determined by the viscosity and the monomer friction coefficient between the polymer and the substrate, k ($k = \eta/b$). That the velocity is constant is associated with the fact that the driving force is constant. Experimentally this may be confirmed by

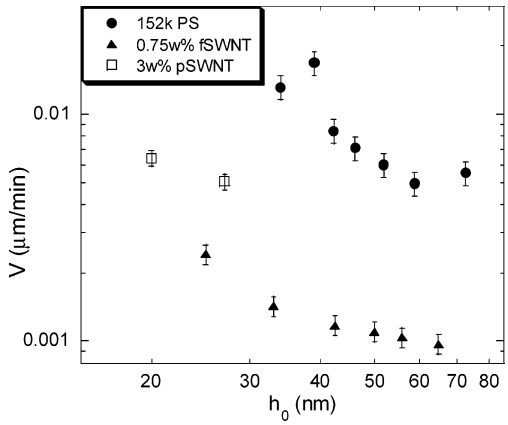

Figure 3. Velocity as a function of film thickness is shown for the 0.75 wt % functionalized SWNT composites, the 3 wt % pristine SWNT composites, and the pure PS.

measuring the dynamic contact angle between the moving front and the substrate (we will return to this issue later). While the radius of the hole increases linearly with time, the width of the rim increases as the square root of time due to a conservation of volume constraint.[44] Eventually as time progresses, the velocity of growth eventually decreases and $R \propto t^{2/3}$.[43,44] The decrease of the growth rate at long times follows from the fact that the frictional resistance increases with the size of the rim while the driving force remains constant.[44] In the second extreme scenario, the resistance to growth is determined entirely by the dissipation of energy within the film. Under these conditions, the growth velocity is also constant, but the velocity does not depend on the film thickness; accordingly, $V \propto |S|/\eta$.[51,52]

Of interest to us in this paper are films of PS and PS-SWNT in the thickness regime where they are metastable. Holes nucleate throughout the films and grow; eventually they form droplets. The droplets that develop on the substrate from the destabilized PS and PS-SWNT films possess the same equilibrium contact angles ($\theta_E = 32 \pm 2°$). The time dependencies of the radii of holes in the Si/SiO_x/PS-functionalized-SWNT systems are plotted in Figure 2. In each case R exhibits a linear dependence on time.

The velocity of hole growth increases with decreasing film thickness, as illustrated in Figure 3 for each system. For thicknesses $h < 50$ nm, $V_{PS-SWNT} \propto h^{-3}$ and $V_{PS} \propto h^{-1}$. These data also indicate that $V_{PS} \approx 5V_{PS-SWNT}$ for $h > 50$ nm. Moreover, $V_{PS}/V_{PS-SWNT}$ increases with decreasing with thickness. This plot, in addition, includes two data points for the nanocomposite film of PS mixed with 3 wt % nonfunctionalized SWNT's. Comparatively, the velocities of hole growth in the samples containing the 3 wt % nonfunctionalized SWNT's exhibit modest changes compared to the effect of the functionalized SWNTs. The data in this figure clearly illustrate the significant effect that functionalized nanotubes have on the dewetting dynamics in polystyrene films.

The differences between the hole-growth velocities, V_{PS} and $V_{PS-SWNT}$, are not associated with differences between the driving forces. In fact, the magnitudes of the driving forces for hole growth in the PS and the PS-SWNT films are similar. Masson and Green[33] reported that the dynamic contact angle, θ_{PS}, for PS was a constant, 5.5°, in the linear growth regime for films in the thickness range $h > 25$ nm. In the nanocomposite thin films, the dynamic contact angle was also $\theta_{PS-SWNT} = 5.5 \pm 1° = \theta_{PS}$ and remained constant throughout the linear region of hole growth. The equilibrium contact angles are also comparable in these systems, $\theta_E = 32 \pm 2°$ for the nanocomposite droplets (Masson and Green found $\theta = 35°$ for PS[33]). Since the driving force for hole growth is [51,52]

$$F_D = \gamma(\cos \theta_E - \cos \theta_D) \tag{2}$$

suggesting that these forces are similar in both systems, then there should be another reason for the dramatic decrease of the hole growth velocity in the PS-SWNT films.

Since there appears to be no evidence of pinning at the line of contact, it is probable that a change in the effective viscosity of the film could account for the 5 differences in hole-growth velocities on these systems. In the thicker film regime where $V_{PS} \approx 5V_{PS-SWNT}$, the viscosities of the thicker films ($h > 50$ nm) should be comparable to the bulk viscosities. Mitchell et al. showed that by adding 0.75 wt % functionalized SWNT's to bulk PS the zero shear viscosity increased by a factor of ~3.[11] It follows from eq 1 that the velocities and the viscosities should be related such that

$$\frac{V_{PS}}{V_{PS-SWNT}} = \frac{\eta_{PS-SWNT}}{\eta_{PS}} \tag{3}$$

This equation suggests that the larger viscosity of the nanocomposite qualitatively accounts for the slower hole-growth rates in these films compared to PS; eq 3 predicts a factor of 3 whereas experimentally a factor of 5 is observed.

The increase of the hole-growth velocity with decreasing h is now addressed in further detail. Theory predicts that the velocity of hole growth should increase with decreasing film thickness as $V \propto h^{-1/2}$, whereas the data indicate that the increase with decreasing h is $V \propto h^{-\alpha}$, where $\alpha \sim 3$ for the PS system and $\alpha \sim 1$ for the PS-SWNT system. The prediction that $V \propto h^{-1/2}$, as mentioned earlier, is based on the notion that the resistance to hole growth is largely associated with the dissipation of energy at the polymer/substrate interface. Also implicit here is that the viscosity of the film, η, remains constant, independent of h. The obvious question, therefore, is what would account for the excess velocity with decreasing h. We begin by reiterating that the driving force is constant. Therefore, one source of the increase of the velocity with decreasing h could be a decrease of the viscosity with decreasing film thickness, $\eta = \eta(h)$. (A change of extrapolation length with film thickness, $b = b(h)$, could be considered, but b is determined by the viscosity.)

Two factors would suggest that the viscosity should increase with decreasing film thickness, which would be at odds with our suggestion that η decreases with decreasing h. First, studies indicate that when the film is confined between two plates, the viscosity increases with decreasing film thickness.[56,57] While these observations would ordinarily support a conclusion that in our system the viscosity may in fact increase with decreasing h, the following point should be considered. At a free surface, the chain segments possess more configurational freedom than in the bulk, and in fact, the segmental dynamics are faster than the bulk.[58] The

interactions in our system are asymmetric, chains interact with a free surface and with a hard, confining, substrate. These relative interactions at the interfaces would strongly influence the viscosity of the system. In this regard the behavior of our system is, in principle, different from the case where the film is confined between two hard substrates. The second factor that would appear to oppose the notion that the viscosity decreases with decreasing h is that the translational diffusion coefficient of chains in the vicinity of a hard substrate are shown to decrease in relation to the bulk.[53−55]

The flows in our system are the result of instabilities, and the moving fronts are driven by capillarity. In light of this, two possibilities for the decrease of the viscosity with decreasing h should be considered. One possibility is shear thinning. The reduction of the viscosity with h due to shear thinning would be less important in the PS-SWNTs films than in PS films because the moving fronts are driven across the substrate at a much slower rate. This would suggest a weaker thickness dependence of the viscosity in the PS-SWNT films, which is consistent with our data.

A second possibility for the viscosity film thickness dependence is a T_g effect. In thin films, the glass transition temperature is known to decrease, or to increase, with decreasing film thickness, depending on the nature of the interactions between the chain segments and the interfaces.[23−31] In cases where the chains interact strongly with the substrate, e.g., hydrogen bonding, the T_g increases with decreasing film thickness, whereas it decreases when the interactions are weak.[23−31] The latter describes the situation for polystyrene on silicon oxide where T_g decreases with decreasing h, at least for the thicknesses examined in this study.[24,26] Different models have been proposed to explain this phenomenon. Some models consider the effect of segmental mobilities near interfaces; others consider the existence of multiple T_gs within the film. One model by Long and co-workers is based on the notion that the density of local regions (domains) of the sample fluctuate at a rapid rates whereas other regions fluctuate slowly.[27,59,60] They introduced a critical density, ρ_c, above which the relaxation of the domains, each occupying a volume v_0, would correspond to the relaxation rate near the glass transition (∼100 s). The glass transition occurs when the slowly relaxing domains of volume v_0 and density larger than ρ_c percolate. Because the percolation threshold is larger in 2D than in 3D, the glass transition should occur at a lower temperature in thin freely standing films relative to the bulk. In the case where one surface is constrained by a substrate, the interactions between the polymer segments and the substrate become important. If the substrate−polymer interactions are sufficiently strong, then the effective fraction of slow domains in the system increases, and this would lead to the situation wherein the T_g of the film is higher than the bulk. If the interactions are weak, then one encounters a situation wherein the T_g decreases with decreasing h. They predict that the change of the T_g is[27,59]

$$\frac{\Delta T_g}{T_g} \approx \beta\left(\frac{a}{h}\right)^{1/\nu} \tag{4}$$

where a is a segmental length and ν is a critical exponent. The magnitude of the parameter β is of order unity; $\beta < 0$ for systems in which the interactions with the substrate are weak, and $\beta > 0$ when they are strong. These predictions are in agreement with experiment. Long and co-workers also show that the viscosity is connected to these shifts in the glass transition, and the viscosity of the film could be approximated as[59]

$$\eta_{\text{film}}(T,h) = \eta_{\text{bulk}}(T - \Delta T_g) \tag{5}$$

where ΔT_g is the magnitude of the depression in T_g at h. If this equation, which provides a link between the film thickness dependence of the glass transition temperature, shown in Figure 4, and the viscosity is true, then it suggests that the viscosity decreases with decreasing film thickness in our system. This decrease of the viscosity with film thickness would qualitatively account for the increase of the hole growth velocity with decreasing film thickness observed in pure PS and in the PS-SWNT system. With regard to the thinner films, the ratio of the velocity of hole growth in PS to that in PS-SWNT, $V_{PS}/V_{PS-SWNT}$, increases with decreasing h as shown in Figure 5. The data in Figure 4 indicate that the T_g of PS decreases at a faster rate with decreasing h than the T_g of the PS-SWNT system. Equation 5 would predict that the viscosity of PS should decrease at a faster rate than that of PS-SWNT.

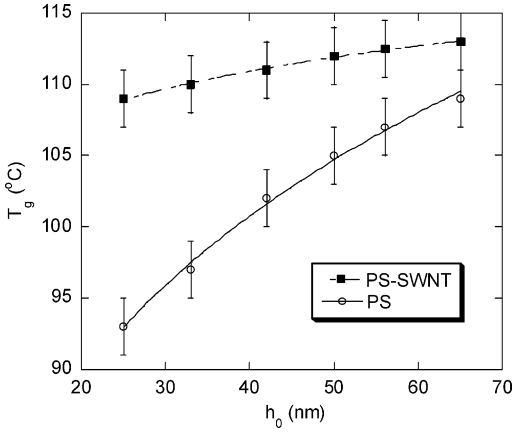

Figure 4. Fitted values of the glass transition temperature for the 0.75 wt % functionalized SWNT composite and the pure PS are shown for various film thicknesses. The T_g values were calculated from fits of the data in ref 31.

With this information regarding $\eta(h)$ and possible connections to the hole growth velocities, it is tempting to use the WLF equation[61] to make a quantitative prediction of the magnitude of the shifts in the growth velocities between both systems. However, accuracy may be in question because the WLF constants, c_1 and c_2, are expected to be film thickness dependent.[62,63] One should in principle be able to perform a temperature-dependent study of the film thickness dependence of the hole growth velocity in order to determine such constants. This would have to be the subject of a separate study. Finally, there remain a number of open issues. The effect of shear thinning on the viscosity in these thin film systems is not fully understood (however, this is unlikely to provide an alternate explanation). On the other hand, independent and reliable measurements show that the glass transition temperature decreases with h, which would support the notion of a decreasing viscosity with decreasing film thickness. These observations would lead one to draw different conclusions regarding the film thickness dependence of the hole-growth velocity and by extension the viscosity. The issue

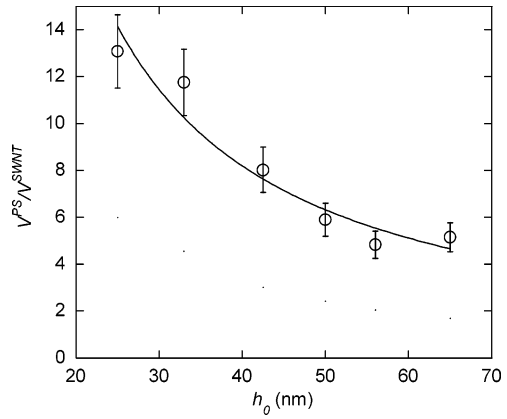

Figure 5. Ratio of the hole growth velocity of the pure PS films to the 0.75 wt % functionalized SWNT films is plotted here.

becomes more complex since reliable studies show that translational diffusion decreases as the film thickness decreases in supported PS films.[53−55] This would argue that the viscosity should increase with deceasing film thickness, as indeed some studies have shown. On the other hand, it might be argued that since the flows in our samples are "driven," then the translational diffusion measurements may not be relevant. Dewetting rates exceed translational diffusion rates. Nevertheless, while the connection between the viscosity and the translational diffusion is well understood in bulk systems, a comprehensive picture is yet to emerge in thin supported films. Our measurements do not resolve these issues; instead, they strongly suggest the need for theoretical guidance in this area. Additional features that complicate the issue further is that in PS films thinner than 25 nm the holes no longer remain circular, indicating the influence of inhomogeneous interactions between the substrate and the polymer. Clearly, any comprehensive theory of dynamics would have to include the effect of chain segment interactions with the substrate. In addition, while it may be possible to rationalize some experimental observations of dynamics in terms of an ensemble averaged T_g, as measured by many techniques, considerations of the influence of a depth dependent $T_g(z)$ on dynamics needs to be considered in future studies.[64]

Conclusion

We have shown that the velocities of hole growth in PS thin films are appreciably larger than hole-growth velocities in PS-SWNT films, $V_{PS} > V_{PS-SWNT}$. In fact, $V_{PS}/V_{PS-SWNT}$ increases from approximately 5 for $h >$ 50 nm to 15 at $h = 25$ nm. Theoretically, the increase of V with decreasing h should be $V \propto h^{-1/2}$. Instead, we measured a much stronger dependence, $V \propto h^{-\alpha}$, where $\alpha \sim 3$ for PS films and $\alpha \sim 1$ for the PS-SWNT films. The lower hole growth rates in the PS-SWNT films is consistent with the notion that the effective viscosities of the nanocomposite films are larger than the viscosities of the pure PS films. The excess film thickness-dependent growth velocities are related to film thickness-dependent viscosities of the films. We also showed that functionalized nanotubes were more effective at reducing the velocities than nonfunctionalized tubes. This result implicates the role of polymer−filler interactions on the dewetting rates of polymer thin films. Finally, our results underscore the need for a comprehensive theory that describes structure and dynamical processes in polymer systems near interfaces.

Acknowledgment. This work was supported by the National Science Foundation (DMR#0072898) and the Robert A. Welch Foundation. The materials were obtained from Ramanan Krishnamoorti, who prepared them using procedures described in ref 11.

References and Notes

(1) Saito, R.; Dresselhaus, G.; Dresselhaus, M. S. *The Physical Properties of Nanotubes*; Imperial College Press: London, 1998.
(2) Besteman, K.; Lee, J.-O.; Wiertz, F. G. M.; Heering, H. A.; Dekker, C. *Nano Lett.* **2003**, *3*, 727.
(3) Rege, K.; Raravikar, N. R.; Kim, D.-Y.; Schadler, L. S.; Ajayan, P. M.; Dordick, J. S. *Nano Lett.* **2003**, *3*, 829.
(4) Kymakis, E.; Amaratunga, G. A. *Appl. Phys. Lett.* **2002**, *80*, 112.
(5) Kempa, K.; Kimball, B.; Rybczynski, J.; Huang, Z. P.; Wu, P. F.; Steeves, D.; Sennet, M.; Giersig, M.; Rao, D. V. G. L. N.; Carnahan, D. L.; Wang, D. Z.; Lao, J. Y.; Li, W. Z.; Ren, Z. F. *Nano Lett.* **2003**, *3*, 13.
(6) Blanchet, G. B.; Fincher, C. R.; Gao, F. *Appl. Phys. Lett.* **2003**, *82*, 1290.
(7) Haggenmueller, R.; Gommans, H. H.; Rinzler, A. G.; Fichser, J. E.; Winey, K. L. *Chem. Phys. Lett.* **2000**, *330*, 219.
(8) Kearns, J. C.; Shambaugh, R. L. *J. Appl. Polym. Sci.* **2002**, *86*, 2079.
(9) Valentini, L.; Biagotti, J.; Kenny, J. M.; Lopez Manchado, M. A. *J. Appl. Polym. Sci.* **2003**, *87*, 708.
(10) Valentini, L.; Biagotti, J.; Kenny, J. M.; Santucci, S. *J. Appl. Polym. Sci.* **2003**, *89*, 2657.
(11) Mitchell, C. A.; Bahr, J. L.; Arepalli, S.; Tour, J. M.; Krishnamoorti, R. *Macromolecules* **2002**, *35*, 8825.
(12) Bahr, J. L.; Tour, J. M. *J. Mater. Chem.* **2002**, *12*, 1952.
(13) Bahr, J. L.; Tour, J. M. *Chem. Mater.* **2001**, *13*, 3823.
(14) Bahr, J. L.; Yang, J. P.; Kosynkin, D. V.; Bronikowski, M. J.; Smalley, R. E.; Tour, J. M. *J. Am. Chem. Soc.* **2001**, *123*, 6536.
(15) Dyke, C. A.; Tour, J. M. *J. Am. Chem. Soc.* **2003**, *125*, 1156.
(16) Nikolaev, P.; Bronikowski, M. J.; Bradley, R. K.; Rohmund, F.; Colbert, D. T.; Smith, K. A.; Smalley, R. E. *Chem. Phys. Lett.* **1999**, *313*, 91.
(17) Binder, K. *Adv. Polym. Sci.* **1994**, *112*, 181.
(18) Binder, K. *Adv. Polym. Sci.* **1999**, *138*, 1.
(19) Russell, T. P. *Curr. Opin. Colloid Interface Sci.* **1996**, *1*, 107.
(20) Fasolka, M. J.; Mayes, A. M. *Annu. Rev. Mater. Res.* **2001**, *31*, 323.
(21) Green, P. F.; Limary, R. *Adv. Colloid Interface Sci.* **2001**, *94*, 53.
(22) Limary, R.; Green, P. F. *Eur. Phys. J. E* **2002**, *8*, 103.
(23) Keddie, J. L.; Jones, R. A.; Cory, R. A. *Faraday Discuss.* **1994**, *98*, 219.
(24) Keddie, J. L.; Jones, R. A.; Cory, R. A. *Europhys. Lett.* **1994**, *27*, 59.
(25) Torres, J. A.; Nealy, P. F.; de Pablo, J. J. *Phys. Rev. Lett.* **2000**, *85*, 3221.
(26) Forrest, J. A.; Dalnoki-Veress, K. *Adv. Colloid Interface Sci.* **2001**, *94*, 167.
(27) Long, D.; Lequeux, F. *Eur. Phys. J. E* **2001**, *4*, 371.
(28) McCoy, J. D.; Curro, J. G. *J. Chem. Phys.* **2002**, *116*, 9154.
(29) Pham, J. Q.; Green, P. F. *J. Chem. Phys.* **2002**, *116*, 5801.
(30) Pham, J. Q.; Green, P. F. *Macromolecules* **2003**, *36*, 1665.
(31) Pham, J. Q.; Green P. F. *J. Polym. Sci.* **2003**, *41*, 3339.
(32) Reiter, G. *Macromolecules* **1994**, *27*, 3046.
(33) Masson, J. L.; Green, P. F. *Phys. Rev. E* **2002**, *65*, 031806.
(34) Israelachvili, J. *Intermolecular and Surface Forces*; Academic Press: New York, 1992.
(35) Sharma, A.; Khanna, R. *Phys. Rev. Lett.* **1998**, *81*, 3463.
(36) Seemann, R.; Herminghaus, S.; Jacobs, K. *Phys. Rev. Lett.* **2001**, *86*, 5534.
(37) Müller, M.; MacDowell, L. G.; Müller-Buschbaum, P.; Wunnike, O.; Stamm, M. *J. Chem. Phys.* **2001**, *115*, 9960.
(38) Brochard-Wyart, F.; Daillant, J. *Can. J. Phys.* **1990**, *68*, 1084.
(39) Reiter, G. *Phys. Rev. Lett.* **1992**, *68*, 75.
(40) Reiter, G. *Langmuir* **1993**, *9*, 1344.
(41) Segalman, R.; Green, P. F. *Macromolecules* **1999**, *32*, 801.
(42) Masson, J. L.; Green, P. F. *Phys. Rev. Lett.* **2002**, *88*, 205504.
(43) Green, P. F.; Ganesan, V. *Eur. Phys. J. E* **2003**, *12*, 449.
(44) Brochard-Wyart, F.; Debregeas, G.; Fondecave, R.; Martin, P. *Macromolecules* **1997**, *30*, 1211.
(45) Barnes, K. A.; Karim, A.; Douglas, J. F.; Nakatani, A. I.; Gruell, H.; Amis, E. J. *Macromolecules* **2000**, *33*, 4177.

(46) Sharma, S.; Rafailovich, M. H.; Peiffer, D.; Sokolov, J. *Nano Lett.* **2001**, *1*, 511.
(47) Cole, D. H.; Shull, K. R.; Baldo, P.; Rehn, L. *Macromolecules* **1999**, *32*, 771.
(48) Luo, H.; Gersappe, D. *Macromolecules* **2004**, *37*, 5792.
(49) Reiter, G.; Sharma, A. *Phys. Rev. Lett.* **2001**, *87*, 166103.
(50) Masson, J. L.; Olufokunbi, O.; Green, P. F. *Macromolecules* **2002**, *35*, 6992.
(51) de Gennes, P. G. *Rev. Mod. Phys.* **1985**, *57*, 827.
(52) Redon, C.; Brochard-Wyart, F.; Rondelez, F. *Phys. Rev. Lett.* **1991**, *66*, 715.
(53) Frank, B.; Gast, A. P.; Russell, T. P.; Brown, H. R.; Hawker, C. *Macromolecules* **1996**, *29*, 6531.
(54) Zheng, X.; Rafailovich, M. H.; Sokolov, J.; Strzhemechny, Y.; Schwarz, S. A.; Sauer, B. B.; Rubinstein, M. *Phys. Rev. Lett.* **1997**, *79*, 241.
(55) Soles, C. L.; Douglas, J. F.; Wu, W.-L.; Dimeo, R. M. *Phys. Rev. Lett.* **2002**, *88*, 037401.
(56) Luengo, G.; Schmitt, F.-J.; Hill, R.; Israelachvili, J. *Macromolecules* **1997**, *30*, 2482.
(57) Semenov, A. N. *Phys. Rev. Lett.* **1998**, *80*, 1908.
(58) Wallace, W. E.; Fischer, D. A.; Efimenko, K.; Wu, W.-L.; Genzer, J. *Macromolecules* **2001**, *34*, 5081.
(59) Long, D.; Sotta, P. Los Alamos National Lab., Preprint Archive, Condens. Matter, 2003; pp 1−33.
(60) Berriot, J.; Montes, H.; Lequeux, F.; Long, D.; Sotta, P. *Europhys. Lett. 64*, 50.
(61) Ferry, J. D. *Viscoelastic Properties of Polymers*; Wiley: New York, 1980.
(62) Zhao, W.; Zhao, M.; Rafailovich, M. H.; Sokolov, J.; Composto, R.; Smith, S. D.; Satkowski, M.; Russell, T. P.; Dozier, W. D.; Mansfield, T. *Macromolecules* **1993**, *26*, 561.
(63) van der Lee, A.; Hamon, L.; Holl, Y.; Grohens, Y. *Langmuir* **2001**, *17*, 7664.
(64) Ellison, C. J.; Torkelson, J. M. *Nature Materials* **2003**, *2*, 695.

MA049008+